Effect of H$_2$ Reduction Temperature on the Properties of Reduced Graphene Oxide and Copper Matrix Composites

Lidong Wang · Ye Cui · Ruiyu Li · Guojian Cao · Bin Li · Weidong Fei

Abstract   Reduced graphene oxide (RGO) and copper composites (RGO/Cu) were successfully fabricated based on a molecular-level mixing method (MLM). The composite powders were reduced in H$_2$ at 350, 450, and 550 °C and then consolidated by spark plasma sintering (SPS) in order to evaluate the effect of H$_2$ reduction temperature on the properties of the composites. The results indicate that the strengths of the composite decrease with the increase of H$_2$ reduction temperature, while the electrical conductivity reaches its maximum at 450 °C and minimum at 550 °C. Hot rolling could benefit the electrical conductivity. The yield strength of the RGO/Cu composite reduced to 337 MPa at 350 °C. The electrical conductivity of the RGO/Cu composite reduced at 450 °C after hot rolling reaches 60.26% IACS. The properties of the RGO/Cu composites can be designed by adjusting the reduction degree of RGO and by hot rolling.

KEY WORDS: Nanostructure; Copper; Composites; Hydrogen; Mechanical properties

1 Introduction

Graphene, consisting of a single to few layers of covalently bonded sp^2 carbon atoms [1], has extraordinary mechanical properties (Young's modulus of ∼1 TPa and tensile strength of ∼130 GPa) [2], remarkable electron mobility (15,000 cm^{2}V^{-1}s^{-1}) [3] and super high thermal conductivity (5,000 Wm^{-1}K^{-1}) [4]. The excellent properties of graphene make it as an excellent candidate reinforcement for different kinds of composites [5, 6]. There are many kinds of methods for the preparation of graphene, such as micromechanical cleavage of graphite [1], laser exfoliation of highly ordered pyrolytic graphite [7], chemical oxidation and reduction method [8], chemical vapor deposition (CVD) [9], and epitaxial growth on SiC [10]. Among them, chemical oxidation and reduction method is versatile and easily scalable, and usually used to produce graphene-based materials [8].

The developments of carbon nanotubes (CNTs) reinforced-composites [11] and graphene reinforced-metal composite [12] have shown great potentiality for improving the multiple properties of metal matrix composites. They could be used widely in the electrical and electronic fields, since they may integrate many properties, such as high strength, excellent electrical conductivity, and high thermal conductivity.

Cha et al. [13] developed a molecular-level mixing method (MLM) for composite powders and fabricated

L. Wang · Y. Cui · B. Li · W. Fei
School of Materials Science and Engineering, Harbin Institute of Technology, Harbin 150001, China

R. Li
Shanghai Institute of Space Power-Sources, Shanghai 200245, China

G. Cao
School of Materials Science and Engineering, Harbin University of Science and Technology, Harbin 150040, China

W. Fei (✉)
School of Mechanical Engineering, Qinghai University, Xining 810016, China
e-mail: wdfei@hit.edu.cn

successfully CNT/Cu composites with molecular-level dispersion by spark plasma sintering. Remarkable enhancement of the compressive strengths of the CNT/Cu composites was found. Hwang et al. produced graphene/Cu composites by MLM and SPS method [14]. The composites have high elastic modulus and yield strength. Kim et al. pointed out that the interfacial oxygen atoms on the surface of CNT could reinforce the interaction between CNT and copper [15]. However, more oxygen atoms on the surface of CNT mean more oxidation of CNT, which may decrease the conductivity of CNT. As a result, the conductivity of the composite may be reduced, which may greatly limit the application of the composites. Similar situation would be encountered for graphene-reinforced copper composites. So far, no effort has been made to evaluate the effect of oxidation of graphene on the strength and electrical conductivity of graphene-reinforced copper composites.

In this work, we produced reduced graphene oxide (RGO)/Cu composites by an improved MLM method. In order to evaluate the effect of H_2 reduction temperature on the properties of the composites, the composite powders were reduced in H_2 at different temperatures and then consolidated by spark plasma sintering (SPS). The compressive strength and the conductivity of the composites were analyzed. The effect of hot rolling was also studied.

2 Experimental

2.1 Sample Preparation

2.1.1 Preparation of Graphite Oxide Colloid

The method used here for graphene oxide was, reported in Ref. [16], by exfoliating graphite oxide in water using ultrasonic treatment. Graphite oxide powder (Nanjing XF Nano Materials Tech Co., Ltd) was dispersed in water to obtain a graphite oxide solution with a concentration of 0.5 mg/mL, which was then treated with a KQ-800KDE ultrasonic cleaner (Kun Shan Ultrasonic Instruments Co., Ltd) for 120 min. At last, a luminous yellow graphene oxide solution was formed.

2.1.2 Fabrication of Composite Powders by Improved MLM Method

The synthesis method for the RGO/Cu composite powder is based on an MLM method that was reported in Ref. [13] but different from it in two aspects: using cuprammonia instead of the alcohol solution of $Cu(CH_3COO)_2 \cdot 2H_2O$ and mixing the solution vigorously by a rotor–stator mixer during drying process. A typical synthesis process of the composite powder is as follows: 46 g of copper acetate

($Cu(Ac)_2 \cdot H_2O$, analytic reagent) was dispersed in 92 mL of ammonia (analytic reagent, 28–29 wt%) to obtain a solution of cuprammonia. The graphene oxide solution (184 mL) was added to the cuprammonia solution and treated with ultrasonic cleaner for 30 min. Then, the solution was dried at 100 °C with the help of the rotor–stator mixer (FA25, Gongyi City Yuhua Instrument CO., LTD), which offers vigorous stirring to the solution. The dried powder was heated at 220 °C in air for 12 h to remove the residual water. At last, the dried powder was reduced at 350, 450, or 550 °C for 2 h at atmospheric pressure in hydrogen gas produced by QL-300 (Shandong Saikesaisi Hydrogen Energy Co., Ltd); then a hydrogen removal process was done at 550 °C in argon for 30 min to eliminate the hydrogen left in the composite powders.

2.1.3 Consolidation of RGO/Cu Composite Powders

The RGO/Cu composite powders were consolidated by SPS at 600 °C for 5 min in a vacuum of 0.1 Pa with an applied pressure of 40 MPa. The volume fraction of graphene in the composite is 2.4%, assuming that graphene oxide has a density of 2.2 g/cm^3. The final sizes of the sintered RGO/Cu composites were 20 mm in diameter and 5 mm in thickness.

The composites were abbreviated as RGO/Cu-350, RGO/Cu-450, and RGO/Cu-550, corresponding to the H_2 reduction temperature of 350, 450, and 550 °C, respectively. Samples of RGO/Cu-450 and RGO/Cu-550 were hot rolled up to a reduction of 60% at 700 °C, and the samples were named as RGO/Cu-450(R) and RGO/Cu-550(R). The densities of the composites were measured by Archimedes method.

2.1.4 Characterization

X-ray diffraction (XRD) analyses were performed on a Philips X'Pert X-ray diffractometer with CuK_α radiation. Raman spectra were preformed from 500 to 3,000 cm^{-1} on a B&W Tek Confocal Micro-Raman spectrometer using a 532 nm laser. Scanning electron microscopy (SEM) analyses were carried out on a Hitachi SU-70 scanning electron microscope. X-ray photoelectron spectroscopy (XPS) was performed on a PHI 5700 ESCA System. Compressive and tensile tests were performed using an Instron 5500R All-purpose Electronic Tester. The crosshead speed was 0.5 mm/min for compressive test and 0.1 mm/min for tensile test at room temperature. The compressive samples had a cylindrical disk shape, 3 mm in height, and 3 mm in diameter. The loading directions are parallel to the pressing direction of SPS. The conductive property was tested by 4-probe method with a 2512B Low DC Resistance Tester (Suzhou Changsheng Electronic Technology Co., Ltd.).
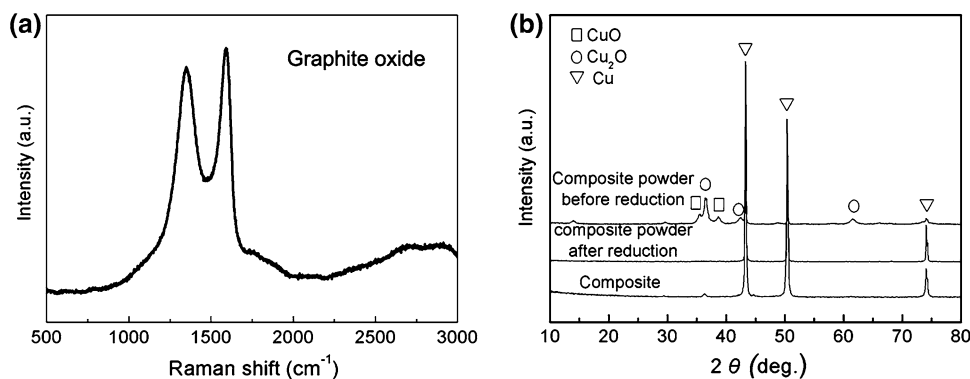
Fig. 1 **a** Raman spectrum of GO; **b** XRD spectra of RGO/Cu-450 composite powders before and after reduction and the RGO/Cu-450 composite

The samples for conductivity tests were cut into sheets with a length of 13 mm, width of 5 mm, and thickness of 0.4 mm.

3 Results and Discussion

Raman spectrum of graphite oxide has a wide D peak (1,350 cm^{-1}) and G (1,594 cm^{-1}) peak, as shown in Fig. 1a. The result shows a typical structure of graphite oxide [17]. The XRD spectra of RGO/Cu-450 composite powder before and after H$_2$ reduction and the RGO/Cu-450 composite are shown in Fig. 1b. The peaks at 2θ of 36.5°, 42.3°, and 61.4° are assigned to (111), (200), (220) crystalline planes of Cu$_2$O (PDF No. 770119), respectively. The peaks at 2θ of 35.5°, 38.7°, and 48.7° are assigned to ($\bar{1}$11), (111) and ($\bar{2}$02) crystalline planes of CuO (PDF No. 801916), respectively. The oxides have been reduced by H$_2$ gas, indicated by the disappearance of the peaks corresponding to CuO and Cu$_2$O after H$_2$ reduction. It can be concluded that H$_2$ reduction is effective to remove the oxides of copper in the composite powder. However, small peaks of Cu$_2$O appeared after sintering by SPS, which shows that slight oxidation of copper happened during SPS process because of its not high vacuum degree.

XPS was used to analyze the state of carbon in the RGO/Cu composites. C1 s XPS spectra of RGO/Cu-350, RGO/Cu-450, and RGO/Cu-550 are shown in Fig. 2. All samples were etched by Ar for 1 min before the measurements and the curves were treated by a Gaussian–Lorentzian fitting after performing a Shirley background correction. The peaks at 284.6, 286.4, 287.8, and 288.9 eV correspond to sp^2 C–C, C–OH, C=O, and O = C–OH, respectively [18]. The contents of oxygen-containing groups are calculated according to the area summation of the peaks corresponding to the oxygen-containing groups with respect to the overall area of the whole peak. It can be found that the contents of oxygen-containing groups decrease from 35% for RGO/Cu-350 to 13% for RGO/Cu-550, suggesting that

graphene oxide is partly reduced by H$_2$ and that the reduction degree increases with the increase of reduction temperature. In addition, there is still a small quantity of oxygen-containing groups in RGO even after reduction at 550 °C. According to XPS analysis, carboxyl group is the main remaining group.

Figure 3a shows the SEM image of RGO/Cu-450 eroded in FeCl$_3$ solution (10 g FeCl$_3$, 2 mL concentrated HCl and 100 mL water) for 5 min. Thin and crumpled RGO sheets can be found on the eroded surface of the composite as directed by white arrows in Fig. 3a, which suggests that the RGO sheets have been distributed homogeneously in the composite. Fractographs of RGO/Cu-350 and RGO/Cu-550 are shown in Fig. 3b, d. The dimples of RGO/Cu-350 are similar to those of RGO/Cu-550, indicating a characteristic of ductile rupture. An enlarged image of the area outlined in Fig. 3b is shown in Fig. 3c, which shows RGO sheets. Both of the fractographs also demonstrate a characteristic of intergranular fracture, since many flat and smooth fracture surfaces can be found in Fig. 3b, d. Moreover, more cracks can be found in Fig. 3d, indicating that the interface strength between RGO and copper of RGO/Cu-550 is lower than that of RGO/Cu-350.

The mechanical properties of the composites were characterized using compressive tests. The yield strength of RGO/Cu-350 (337 MPa) is two times higher than that of copper [13], indicating that RGO has good reinforcing effect on copper matrix composites. It can be found that the yield strengths of RGO/Cu-350, RGO/Cu-450, and RGO/Cu-550 decrease with the increase of H$_2$ reduction temperature. So the strength of the composites is closely related with the oxidation level of graphene, the lower the oxidation level, and the lower the strength.

The hardness values of RGO/Cu-350, RGO/Cu-450, and RGO/Cu-550 are 109, 108, and 88 HV, respectively, as shown in Fig. 4c. The hardness of pure copper with a grain size of 1,350 nm is 63 HV [19], which is only about 60% of that of the RGO/Cu-350 composite. The hardness values also decrease with the increase of H$_2$ reduction temperature. The
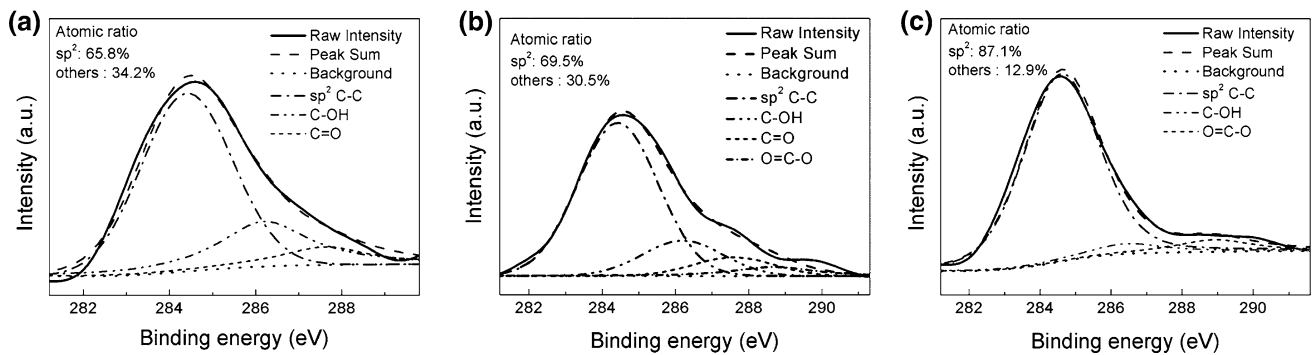
Fig. 2 C1 s XPS spectra of the composites: **a** RGO/Cu-350; **b** RGO/Cu-450; **c** RGO/Cu-550
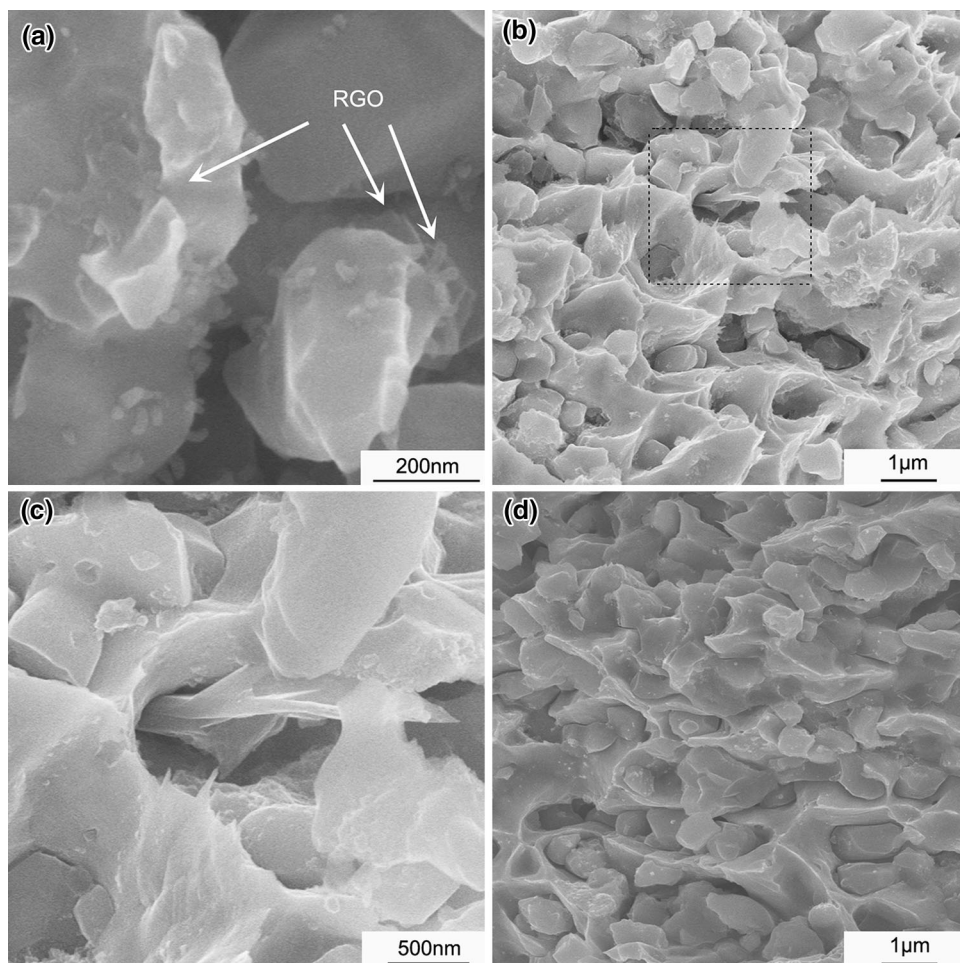

Fig. 3 SEM of the surface of RGO/Cu-450 **a**, fractographs of RGO/Cu-350 **b**, **c**; RGO/Cu-550 **d**

effect of H_2 reduction temperature on the hardness of the composite is similar to that for the compressive test.

The stress–strain curve obtained from the tensile test of RGO/Cu-550(R) is shown in Fig. 4d. The tensile strength is 246 MPa, about 1.4 times higher than that of unreinforced copper produced by SPS [11].

The reason for the decrease of the strength and hardness with the increase of reduction temperature may be

explained as follows. It has been reported that the reaction between carboxyl or hydroxyl groups (O=C–OH), C=O, –OH) and copper atoms can produce Cu–oxygen bonds; these bonds at the interface in CNT/Cu nanocomposites are the origin for an optimized CNT/Cu interface, which helps to transfer the load from the Cu matrix to the CNTs and reinforce the CNT/Cu nanocomposites [15]. The reinforcing mechanism of the RGO/Cu composites would be
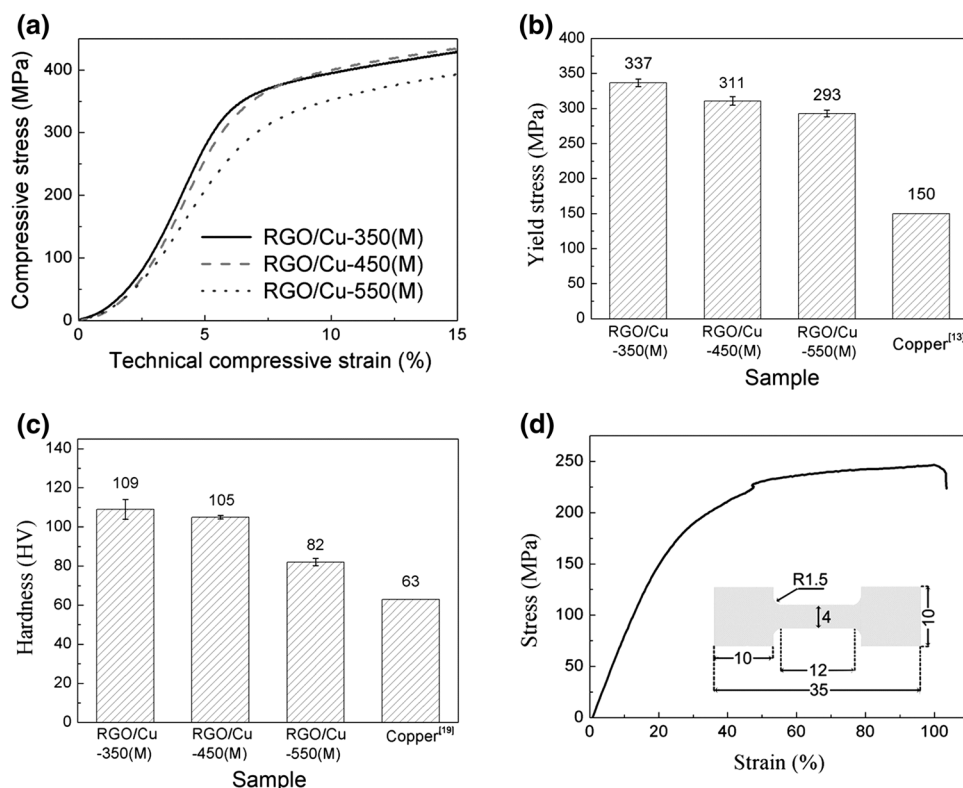
Fig. 4 Mechanical properties of the composites: **a** compressive stress–strain curves of composite with different H2 reducing temperature; **b** compressive stress of composites; **c** hardness of composites; **d** tensile stress–strain *curve* of RGO/Cu-550(R), the *inset* shows the dimensions (in mm) of tensile sample

similar to that of CNT/Cu since the surface of graphene oxide also has carboxyl or hydroxyl groups, which can react with copper atoms. The bonding strength of the interface, a key factor for the mechanical properties of the composites, is closely related with the content of oxygen-containing groups. The XPS analysis suggests that more oxygen-containing groups could be reduced with the increase of reduction temperature, consistent with the previous result that an increase in temperature could facilitate the thermal deoxygenation of graphite oxide [20]. Consequently, the bonding strength of the interface decreases with the increase of reduction temperature, resulting in the decrease of the compressive strength and hardness of the composites.

The conductivities of the composites expressed by IACS (international annealed copper standard) are shown in Fig. 5. It can be seen that the conductivity of RGO/Cu-450 (53.18% IACS) is the highest among those of the three composites reduced at different temperature. In order to understand the change of the conductivity, the measured results of relative density show that the relative densities of RGO/Cu composites with reduced temperatures of 350, 450, and 550 °C are 87.3%, 93.5%, and 88.9%, respectively. It is worth noting that the variation trend of the conductivity increases at first and then decreases, which is
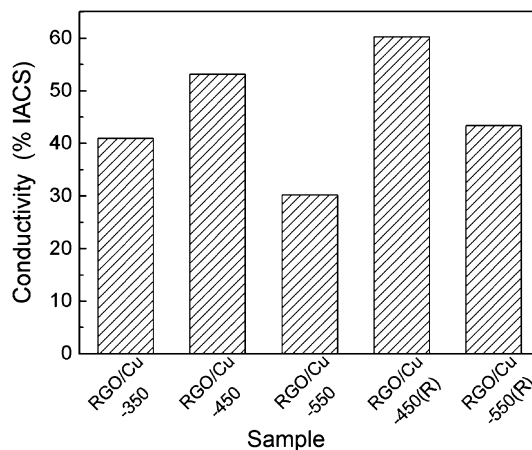

Fig. 5 Conductivities of RGO/Cu composites

similar with that of the density for the composites reduced at 350, 450, and 550 °C, suggesting that the density of the composite is the key factor for the change of the conductivity.

It can be found that the conductivities of the composites treated by hot rolling (RGO/Cu-450(R) and RGO/Cu-550(R), relative density are 95.8% and 88.5%, respectively) are higher than that of the composites before hot

L. Wang *et al.*: Acta Metall. Sin. (Engl. Lett.), 2014, **27**(5), 924–929

929

rolling. So hot rolling can improve the electrical conductivity of the composites. The effect of hot rolling can be understood in two aspects. Firstly, the process of hot rolling could decrease the porosity of the composites and get the micro-cracks healed. Secondly, the recrystallization and grain orientation of copper during hot rolling could benefit the electrical conductivity of the composite. All these could make the composite obtain a better electrical conductivity after hot rolling.

It is interesting to find that the strength and hardness decrease with the increase of H_2 reduction temperature, however, the conductivity is related with the density of the composite and the hot rolling process. These results suggest that the properties of the RGO/Cu composites can be designed by adjusting the reduction content of RGO; in addition, the balance of mechanical properties and the conductivity should be considered in the design process.

4 Conclusions

In summary, RGO/Cu composites with homogenously dispersed RGO sheets within the Cu matrix were successfully fabricated by an improved molecular-level MLM. The relationship between the H_2 reduction temperature of the composite powders and the properties of the composites was discussed. It shows that as the temperature increases from 350 to 550 °C, the compressive strengths decrease, however, the electrical conductivity of the composites increases at first and then decreases. Hot rolling could benefit the electrical conductivity of the composites. The properties of the RGO/Cu composites can be designed by adjusting the reduction degree of RGO and by hot rolling.

References

[1] K.S. Novoselov, A.K. Geim, S.V. Morozov, D. Jiang, Y. Zhang, S.V. Dubonos, I.V. Grigorieva, A.A. Firsov, Science **306**, 666 (2004)
[2] C. Lee, X.D. Wei, J.W. Kysar, J. Hone, Science **321**, 385 (2008)
[3] J.H. Chen, C. Jang, S.D. Xiao, M. Ishigami, M.S. Fuhrer, Nat. Nanotechnol. **3**, 206 (2008)
[4] A.A. Balandin, S. Ghosh, W.Z. Bao, I. Calizo, D. Teweldebrhan, F. Miao, C.N. Lau, Nano Lett. **8**, 902 (2008)
[5] A.K. Geim, K.S. Novoselov, Nat. Mater. **6**, 183 (2007)
[6] Z. Chen, W.C. Ren, L.B. Gao, B.L. Liu, S.F. Pei, H.M. Cheng, Nat. Mater. **10**, 424 (2011)
[7] M. Qian, Y.S. Zhou, Y. Gao, J.B. Park, T. Feng, S.M. Huang, Z. Sun, L. Jiang, Y.F. Lu, Appl. Phys. Lett. **98**, 173108 (2011)
[8] D.Y. Cai, M. Song, C.X. Xu, Adv. Mater. **20**, 1706 (2008)
[9] M. Wang, S.K. Jang, W.J. Jang, M. Kim, S.Y. Park, S.W. Kim, S.J. Kahng, J.Y. Choi, R.S. Ruoff, Y.J. Song, S. Lee, Adv. Mater. **25**, 2746 (2013)
[10] J. Hwang, M. Kim, V.B. Shields, M.G. Spencer, J. Cryst. Growth **366**, 26 (2013)
[11] K. Kim, S. Cha, S. Hong, Mater. Sci. Eng. A **430**, 27 (2006)
[12] Y. Kim, J. Lee, M.S. Yeom, J.W. Shin, H. Kim, Y. Cui, J.W. Kysar, J. Hone, Y. Jung, S. Jeon, S.M. Han, Nat. Commun. **4**, 3114 (2013)
[13] S.I. Cha, T.K. Kim, S.N. Arshad, C.B. Mo, S.H. Hong, Adv. Mater. **17**, 1377 (2005)
[14] J. Hwang, T. Yoon, S.H. Jin, J. Lee, To Kim, S.H. Hong, S. Jeon, Adv. Mater. **25**, 6724 (2013)
[15] K.T. Kim, S.I. Cha, T. Gemming, J. Eckert, S.H. Hong, Small **4**, 1936 (2008)
[16] S. Stankovich, D.A. Dikin, R.D. Piner, K.A. Kohlhaas, A. Kleinhammes, Y. Jia, Y. Wu, S.T. Nguyen, R.S. Ruoff, Carbon **45**, 1558 (2007)
[17] K.N. Kudin, B. Ozbas, H.C. Schniepp, R.K. Prud'homme, I.A. Aksay, R. Car, Nano Lett. **8**, 36 (2008)
[18] D. Yang, A. Velamakanni, G. Bozoklu, S. Park, M. Stoller, R.D. Piner, S. Stankovich, I. Jung, D.A. Field, C.A. Ventrice, R.S. Ruoff, Carbon **47**, 145 (2009)
[19] M.R. Akbarpour, E. Salahi, F. Alikhani Hesari, A. Simchi, H.S. Kim, Mater. Sci. Eng. A **572**, 83 (2013)
[20] C. Mattevi, G. Eda, S. Agnoli, S. Miller, K.A. Mkhoyan, O. Celik, D. Mostrogiovanni, G. Granozzi, E. Garfunkel, M. Chhowalla, Adv. Funct. Mater. **19**, 2577 (2009)